A Surface-Constrained Volumetric Alignment Method for Image Atlasing

Hao-Chiang Shao*, Wen-Liang Hwang
Institute of Information Science
Academia Sinica
Taiwan
Email: shao.haochiang@gmail.com; whwang@iis.sinica.edu.tw

Yung-Chang Chen
Department of Electrical Engineering
National Tsing Hua University
Taiwan
Email: ycchen@ee.nthu.edu.tw

***Abstract*—In this paper, we propose a prototype system capable of incorporating 3D shape information with conventional TPS-based (thin-plate-spline) volumetric registration method for image atlasing. Our method consists of two phases. The former phase registers and warps the 3D mesh surface models describing the tissue shape boundary of the input image volumes, and the latter aims to align the input image volumes with the aid of the boundary constraints suggested by the former. The proposed volumetric registration method is driven and constrained by the pre-registered 3D mesh surface model. Experiments show that using our framework for volumetric image registration and warping obtains a performance comparable to or better than a well-known benchmark method.**

I. Introduction

Brain research requires a standardized brain atlas, which can act as a calibrated space to accommodate neural images acquired from different preparations, to describe both the variance and invariance in brain anatomy and neuron connectivity. To develop a brain atlas and to accommodate images into a calibrated space—that is, image atlasing—will require techniques adapted from average brain model construction methods and image registration/warping schemes. Recent techniques [1], [2], [3], [4], [5] have made it feasible to construct a 2D+Z or a 3D single standard brain model or to align images acquired with the same stain process and image settings. These techniques already form a beltline for warping images, acquired by the same stain process and imaging conditions, into a standardized space representative of a certain organ/tissue, e.g., Drosophila adult brain [4], [6]. Although techniques of aligning—registering and warping—images acquired by the same way has been getting mature, little research has addressed how to align images acquired by different sample preparation and stain processes, e.g., images acquired by different labs.

Aligning microscopic images acquired by different stain process and image setting is a multimodality registration problem in some sense. It is hard to handle such registration tasks, because the registration accuracy may be affected by the differences in image properties between the to-be-aligned image sets. Figure 1 shows an example of such difficulty. In this experiment, the input source images were stained against DLG (Drosophila large discs) and imaged within FocusClear, so the neuropil shape boundaries, as well as the image brightness and the contrast, differ from those in reference target images prepared using NC82, such as images from the FlyLight database and the reference brain images downloaded from BrainAligner's website. We can notice that the shape boundary of the registration result shown in Figure 1(c) is obviously distorted.

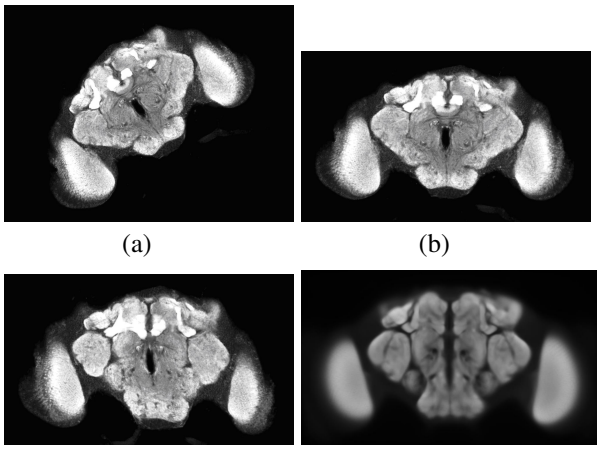

Fig. 1. Aligning images acquired by different stain processes and imaging setting. (a) the 22th slice of the input image stack. (b) warping result after global registration. (c) warping result after local registration. (d) the 70th slice the of reference target image volume. This experiment was performed by BrainAligner [4].

The primary reason to this phenomenon is the lack of suitable boundary conditions for the volume registration process. Because common registration strategies operate in a 2D+Z manner rather than 3D, it usually presents a difficulty in assuring the depth correspondence between any two image stacks. If the Z-correspondence is not guaranteed, it will be difficult to ascertain the fidelity of feature correspondence and boundary conditions. Moreover, one another concern is that biological samples may be rotated. No matter how accurately technicians mount sample tissues, e.g., *Drosophila* brains, no true Z-correspondence can be found without accounting for the possible rotations first. Consequently, we plan to overcome this difficulty by introducing the 3D mesh

surface model (or the 3D calibrated space) into conventional 2D+Z registration and warping framework. Our idea can be described as below:

Let f_b be the mapping function used to transform an image volume $\mathbf{I}_b$ acquired by Lab-B *into the atlas (or the standardized space)* S_b*, and let $\Pi_{A\to B}$ be the mapping from the atlas* S_a *developed by* Lab-A *to* S_b*. The process of aligning $\mathbf{I}_b$ into* S_a *can be theoretically represented by*

$$(\Pi^{-1}_{A\to B} \circ f_b)(\mathbf{I}_b). \quad (1)$$

Note that when $\mathbf{I}_b$ is the 3D mesh surface model reconstructed from the tissue shape boundary of volume $\mathbf{I}_b$'s slices, the f_b is defined to be identity.

To carry out the process depicted by the above equation, there are at least three indispensable components. First, a standardized 3D mesh model, S, that acts as a calibrated space to accommodate the images acquired by a lab has to be defined. Second, a model-to-model metamorphism scheme that can quantitatively characterize how a 3D model deforms to another, that is $\Pi_{A\to B}$, has to be built. Third, the way to estimate $\Pi^{-1}_{A\to B} \circ f_b$ has to be developed; specifically speaking, a model-driven non-linear registration/warping approach that can map image volumes from one calibrated space into another based on the boundary condition provided by the deformed 3D standard model is required for this purpose.

Because techniques required for the first and second components are already developed, e.g., [1], [2], [5] for the standard atlas construction and [7], [8] for the model metamorphism, we aim in this paper to propose a prototype system for deriving the third component. In order to verify our idea first, we chose two suitable (*Drosophila* brain) image volumes and generated mesh surface models of the external brain surface by **Amira** (a commercial software) so the two mapping function f_b and f_a are defined to be identity. We add an additional boundary constraint, which is suggested by 3D deformed mesh surface model, into conventional 2D thin-plate-spline (TPS) based framework to derive the deformation filed for warping. Hence, the concept of our prototype system is straightforward, and the algorithm itself is easily-implemented.

II. Framework

In order to incorporate additional boundary conditions with conventional volumetric image registration and warping scheme, the proposed prototype system is implemented in two stages. The former stage, surface model alignment stage, first develops the correspondence between the 3D surface models of two to-be-aligned image volumes. Then, the letter, volumetric registration and warping stage, derives the deformation filed and warp the source image volume to the target based on thin-plate-spline model and the additional boundary conditions suggested by the former.

Additionally, because this work focuses on how to derive boundary conditions based on the 3D surface model, we have to note that the correspondences of features locating on 2D slices is assume to be derived by any existing algorithms or assigned manually according to biological requirements. Also note that the both S_a and S_b used in our experiment are the 3D surface model reconstructed from the input image volumes rather than an actual calibrated atlas space, so the mapping f_b and f_a are identity and can be ignored in our experiment. The flowchart of the proposed system is illustrated in Fig. 2.

III. Method

A. Surface Model Alignment

The first stage consists of three primary steps: (1) surface reconstruction, (2) surface correspondence construction, and (3) anchor points extraction.

As for the surface reconstruction step, the surface models S_a and S_b of the to-be-aligned two image volumes can be generated by any meshing algorithm, e.g., [9] or software, e.g., Amira and Avizo. The input of a surface reconstruction method is generally a stack of labeled images—regions enclosed by the shape boundary are manually set to be 1, and regions outside are set to be 0.

Second, the second step aims to register and warp the surface model of input image volume into that of the target image volume and then derive $\Pi_{A\to B}$. There are several mesh morphing or mesh surface registration methods that can be used to derive the mapping between two meshes. The method described in [8] can generate a morphing sequence by developing a hierarchical multiresolution mapping function between two input mesh models. The method described in [10] can transform meshes of the same gynus type yet with different numbers of vertices and faces into meshes sharing the same topological information, i.e., the adjacency information describing relationship between all vertices, edges, and faces; therefore, it is straightforward to derive a one-to-one correspondence between vertices of remeshed models. In this paper, we adopted the method described in [11] to align the surface models of *Drosophila* whole brain, and then we extracted some anchor points from the deformed surface model for the registration procedure in Phase-2.

In the third step of Phase-1, for each selected anchor point v_i^b on S_b, its corresponding points on S_a is found by using

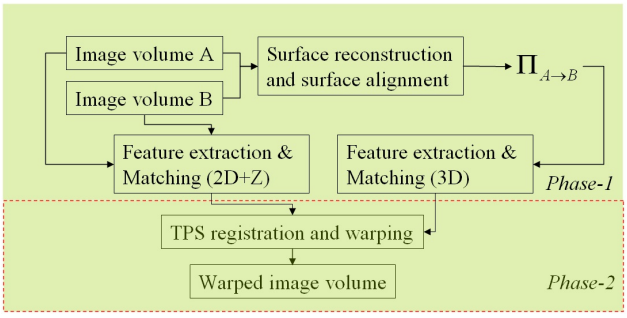

Fig. 2. The block diagram of the proposed system.

$\Pi_{A\to B}$. If a user-specified anchor point is not a vertex of S_b and locates within a triangular patch, e.g., $\Delta v_1 v_2 v_3$, its corresponding point on S_a can be represented as

$$\Pi^{-1}_{A\to B}(v_i^b) = \alpha\Pi^{-1}_{A\to B}(v_1) + \beta\Pi^{-1}_{A\to B}(v_2) + \gamma\Pi^{-1}_{A\to B}(v_3), \quad (2)$$

given that α, β, and γ are the barycentric coordinate of v_i^b with respect to $\Delta v_1 v_2 v_3$.

B. TPS Registration

Given K pairs of corresponding landmarks $\mathbf{v}_i$ and $\mathbf{y}_i$, $i = 1, \cdots, n$ in spaces of dimension d, the TPS registration aims to find a continuous transformation $\mathcal{T} = \mathrm{R}^D \to \mathrm{R}^D$ minimizing a given objective function and fulfill the interpolation conditions [12], [13]

$$\mathbf{y}_i = \mathcal{T}(\mathbf{v}_i), \ i = 1, \cdots, n. \quad (3)$$

Based on the objective function and results given in [13], the analytic solution for any interior point $\mathbf{x} = [x, y]^T$ could be approximated as

$$\mathcal{T}(\mathbf{x}) = \sum_{j=1}^{D+1} d_j \psi_j(\mathbf{x}) + \sum_{i=1}^{K} w_i U(\mathbf{x}, \mathbf{v}_i) \quad (4)$$

with basis functions $U(\mathbf{x}, \mathbf{v}_i)$. The basis functions $U(\mathbf{x}, \mathbf{v}_i)$ span the n-dimensional space depending on landmarks $\mathbf{v}_i$, and the null space is spanned by $\phi_1(\mathbf{x}) = 1$, $\phi_2(\mathbf{x}) = x$, $\phi_3(\mathbf{x}) = y$, and $\phi_3(\mathbf{x}) = z$. Meanwhile, coefficients d_j and w_i in Eq. (4) can be solved by the following linear equations:

$$\mathbf{\Phi d} + \mathbf{K w} = \mathbf{Y} \quad (5)$$

$$\mathbf{\Phi}^T \mathbf{w} = \mathbf{0}, \quad (6)$$

where $K_{i,j} = U(\mathbf{v}_i, \mathbf{v}_j)$, $\Phi_{i,j} = \psi_j(\mathbf{v}_i)$, and $\mathbf{Y}$ is the column vector of one component of the coordinates of landmarks $\mathbf{y}_i$ of the to-be-registered source data. The condition $\mathbf{\Phi}^T\mathbf{w} = 0$ represents the boundary conditions and ensures that the elastic part of the transformation is zero at infinity. $U(\mathbf{x}, \mathbf{v}_i)$ is usually a radial basis functions of the following form:

$$U(\mathbf{v}, \mathbf{y}) = \|\mathbf{v} - \mathbf{y}\|^2 log\|\mathbf{v} - \mathbf{y}\|. \quad (7)$$

Moreover, note that Eq.(5) can be modified as

$$\mathbf{\Phi}\alpha + (\mathbf{K} + \lambda\,\mathbf{W}^{-1})\mathbf{w} = \mathbf{Y}, \quad (8)$$

where $\lambda \geq 0$ is a regularization term used to control the smoothness of the deformation field, and each non-zero entry of the diagonal matrix $\mathbf{W}^{-1}$ is a weighting coefficient representing the landmark (feature) localization error. Consequently, by dividing TPS landmarks into two groups, i.e., a set of anchor points suggested by surface model and a set of internal feature points extracted from 2D image slices, we can then give each group of landmarks a different weighting via $\mathbf{W}^{-1}$, and we then can force the transformation $\mathcal{T}$ to fit the shape boundary while giving a larger tolerance on localization errors of internal feature points.

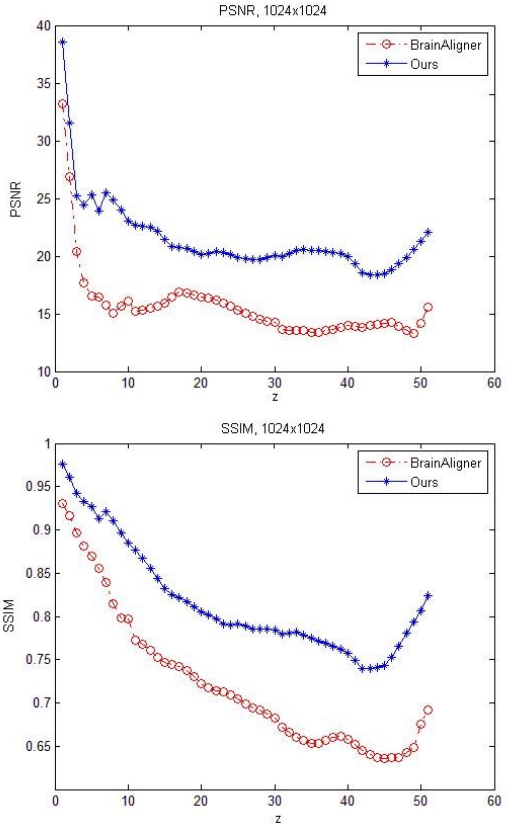

Fig. 3. The PSNR and SSIM of the warped image volume. This experiment is performed by first registering and warping an image stack, namely stack-B, to a reference one, namely stack-A, and then measuring the slice-to-slice PSNR between the warping result and stack-A. The horizontal axis denotes the slice (depth) index.

C. Troubleshooting

The matrix $\mathbf{\Phi}$ may be badly scaled and have a large condition number if the image width or the image height of the input volume is much greater than the number of image slices. To solve this problem, we scaled down the landmark coordinates during the computation to avoid deriving an improper $\mathcal{T}$; then, the landmark coordinates were scaled up while evaluating the deformation field based on the obtained $\mathcal{T}$. Take the image volume we used in our experiment for example. The dimension of the image volume is $1,024 \times 1,024 \times 70$, and the constant factors we selected for x-, y-, and z-coordinates are respectively 100, 100, and 10.

IV. EXPERIMENT RESULTS

Because the image data processed by BrainAligner are not available for download from the FlyLight database, we used the confocal image stacks provided by *FlyCircuit* database [6] to evaluate the performance of our method. We aligned two focal stacks by using BrainAligner and our method to

verify whether the additional constraint suggested by the mesh surface model works. As shown in Fig. 3, the performance of our method is better than that of BrainAligner. Additionally, because the inverse transform of the TPS deformation field may not exist, we used the inpainting method described in [14] to fill up all missing pixels, whereas BrainAligner interpolated the deformation field, rather than interpolate missing pixels' values directly, to circumvent the problem of interpolating missing pixels. Finally, shown in Fig. 4 are the warped images derived by our method and BrainAligner. Because BrainAligner interpolates the deformation field and then warps the images, it usually produces a smooth, continuous, and seamless warping result. However, we deem that in such biomedical image registration/warping problems, one should retain individuality while warping. Please focus on the optical lobe near the lower-left corner of each sub-figures in Figure-4. There is a scar, or a gash, or maybe a mark (the dark, concave region) at the lower-left optical lobe's boundary in Figure-4(a). Our warping result shown in Fig. 4(c) demonstrates that this anatomical feature is retained, whereas it is over-smoothened by BrainAligner.

As for the time complexity, it cost about 68 hours to register and warp an $1,024 \times 1,024 \times 70$ image volume into another by using BrainAligner, whereas the proposed method took about 12 days to generate the warping result based on about 1,000 feature pairs. For a image database containing thousands of image volumes—e.g., there are about $16,000$ image sets on FlyCircuit database—both our method and BrainAligner are too time-consuming to be applicable. Consequently, a necessary future improvement of our method is to reduce the computation time.

V. CONCLUSION

In this paper, we proposed a TPS-based registration method, which is constrained and driven by a pre-aligned mesh surface model, to align image volumes, and the experiments show that the atlasing results are satisfactory. The contributions of proposed system is that it integrates the boundary condition suggested by 3D shape information into conventional TPS volumetric registration method, and hence a better deformation field can then be derived.

Moreover, there are one possible future extension and one future improvement of the proposed system. The future improvement is to reduce the computational time complexity. It may be achieved by some divide-and-conquer strategy: divide input image volume into several overlapped sub-volumes first, design some continuity constraint on the overlapped regions, and then find the transformation/warping functions for all sub-volumes in parallel. The future extension is to make this prototype system adaptive to registration/warping problem of arbitrary f (see Eq.(1)), and we are looking forward to applying our method on cross-lab images data alignment/integration problems.

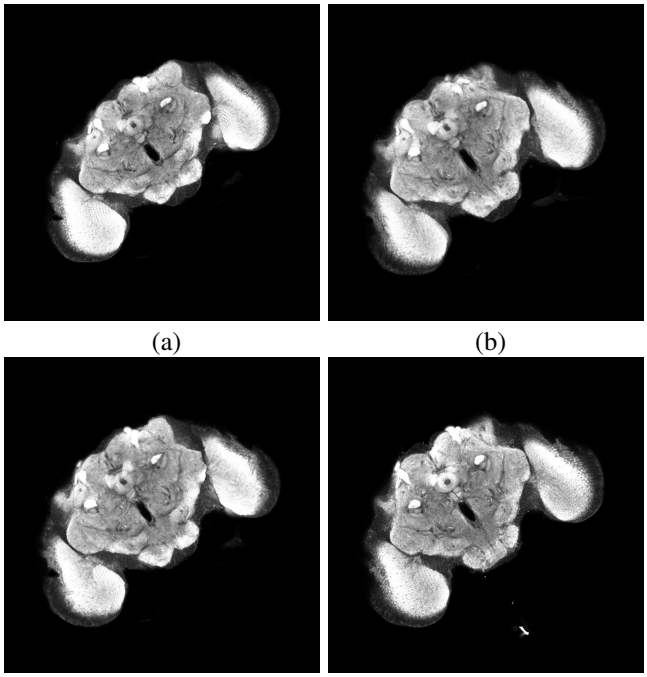

Fig. 4. Comparison of the 25^{th} slices produced by two methods. (a) the input image, (b) the image derived by BrainAligner, (c) the image derived by the proposed method, and (d) the reference image

REFERENCES

[1] K. Rein, M. Zockler, M. T. Mader, C. Grubel, and M. Heisenberg, "The drosophila standard brain," *Curr. Biol.*, vol. 12, pp. 227–231, 2002.

[2] T. Rohlfing, R. Brandt, Calvin R. Maurer Jr., and R. Menzel, "Bee brains, b-splines and computational democracy: generating an average shape atlas," in *Proceedings of the IEEE Workshop on Mathematical Methods in Biomedical Image Analysis, MMBIA, Kauai, Hawaii*, December 2001, pp. 187–194.

[3] A. Jenett, G. M. Rubin, T. Ngo, D. Shepherd, C. Murphy, H. Dionne, B. D. Pfeiffer, A. Cavallaro, D. Hall, J. Jeter, et al., "A gal4-driver line resource for¡ i¿ drosophila¡/i¿ neurobiology," *Cell reports*, 2012.

[4] H. Peng, P. Chung, F. Long, L. Qu, A. Jenett, A. M. Seeds, E. W. Myers, and J. H. Simpson, "Brainaligner: 3d registration atlases of drosophila brains," *Nature methods*, vol. 8, no. 6, pp. 493–498, 2011.

[5] H.-C. Shao, C.-C. Wu, G.-Y. Chen, H.-M. Chang, A.-S. Chiang, and Y.-C. Chen, "Developing a stereotypical *Drosophila* brain atlas," *IEEE Transactions on Biomedical Engineering*, vol. 61, no. 12, pp. 2848–2858, 2014.

[6] "FlyCircuit," *http://www.flycircuit.tw/.*

[7] D. Cohen-Or, A. Solomovic, and D. Levin, "Three-dimensional distance field metamorphosis," *ACM Transactions on Graphics*, vol. 17, no. 2, pp. 116–141, 1998.

[8] A. Lee, D. Dobkin, W. Sweldens, and P. Schröder, "Multiresolution mesh morphing," in *Proceedings of the 26th annual conference on Computer graphics and interactive techniques*. ACM Press/Addison-Wesley Publishing Co., 1999, pp. 343–350.

[9] Y.-C. Chen, Y.-C. Chen, A.-S. Chiang, and K.-S. Hsieh, "A reliable surface reconstruction system in biomedicine," *Computer methods and programs in biomedicine*, vol. 86, no. 2, pp. 141–152, 2007.

[10] H.-C. Shao, W.-L. Hwang, and Y.-Chang Chen, "A backward wavelet remesher for level of detail control and scalable coding,"

in *Proceedings of the IEEE International Conference on Image Processing (ICIP) 2014*.

[11] H.-C. Shao, C.-C. Wu, L.-H. Hsu, W.-L. Hwang, and Y.-C. Chen, "3d thin-plate spline registration for drosophila brain surface model," in *Proceedings of the IEEE International Conference on Image Processing (ICIP) 2013*.

[12] F. Bookstein, "Principal warps: Thin-plate splines and the decomposition of deformations," *IEEE Trans. Pattern Anal. Mach. Intell.*, vol. 11, no. 6, pp. 567–585, 1989.

[13] K. Rohr, H. Stiehl, R. Sprengel, T. Buzug, J. Weese, and M. Kuhn, "Landmark-based elastic registration using approximating thin-plate splines," *IEEE Trans. Med. Imag.*, vol. 20, no. 6, pp. 526–534, 2001.

[14] H. Noori and S. Saryazdi, "Image inpainting using directional median filters," in *International Conference on Computational Intelligence and Communication Networks (CICN), 2010*. IEEE, 2010, pp. 45–49.

[15] G.-Y. Chen, C.-C. Wu, H.-C. Shao, H.-M. Chang, A.-S. Chiang, and Y.-C. Chen, "Retention of features on a mapped drosophila brain surface using a bezier-tube-based surface model averaging technique," *IEEE Trans. Biomed. Eng.*, vol. 59, no. 12, pp. 3314–3326, dec. 2012.

[16] A. Jenett, J. Schindelin, and M. Heisenberg, "The virtual insect brain protocol: creating and comparing standardized neuroanatomy," *BMC Bioinformatics*, vol. 7, no. 1, pp. 544, 2006.

[17] H. Chui and A. Rangarajan, "A new point matching algorithm for non-rigid registration," *Computer Vision and Image Understanding*, vol. 89, no. 2, pp. 114–141, 2003.

[18] A.-S. Chiang, "Aqueous tissue clearing solution," Oct. 29 2002, US Patent 6,472,216.

[19] Y.-C. Liu and A.-S. Chiang, "High-resolution confocal imaging and three-dimensional rendering," *Methods*, vol. 30, no. 1, pp. 86–93, 2003.

[20] K. Chung and K. Deisseroth, "Clarity for mapping the nervous system," *Nature methods*, vol. 10, no. 6, pp. 508–513, 2013.